

Mass properties factors in achieving stable imagery from a gimbal mounted camera

Daniel R. Otlowski, Kurt Wiener, Brandon A. Rathbun
Space Electronics LLC, 81 Fuller Way, Berlin, CT, USA 06037

ABSTRACT

Mass properties play a role in affecting the stability of gimballed imaging platforms. The relationship between static balance and jitter, in some measure, is previously established. The definition and role of dynamic unbalance however, is not as thoroughly understood. Leading to the discussion of dynamic unbalance, we show through the use of analytical means, the jitter resulting from static unbalance generated forces when we follow these forces through the isolation mounting, servo pointing accuracy and disturbance rejection systems using a single degree of freedom model. We then apply the qualitative results to the discussion of dynamic unbalance exploring some of the nuances of product of inertia and cross coupling response. We will offer strategies and specific methods for measuring and correcting static unbalances and the principles of reducing dynamic unbalance in gimbals in order to reduce disturbance response and ultimately improve the image resolution. Finally, we will test a method for measuring and correcting dynamic unbalance to facilitate future quantitative testing aimed toward jitter improvement.

Keywords: Gimbal, balancing, center of gravity, moment of inertia, imaging, jitter, acceleration, MTF, dynamic balance, POI, CG, MOI, stability, product of inertia

1. INTRODUCTION

Gimballed imaging systems are often subject to severe operational acceleration environments. The high power to mass ratio of a small UAV powered by a reciprocating piston engine, and the demanding environment of a helicopter based imaging platform, are two such examples of high vibration applications. These accelerations have an adverse effect on imaging system performance. When the CG is not aligned with the torque motor axes, the undesired moments developed under acceleration will tax the stabilization controls, affect pointing accuracy, and ultimately cause image jitter. When the CG is aligned, the image stabilizes. Physical balancing of assemblies used in high g environments is the only method that transcends all other stabilization methods. It is fundamental. All other compensation arrangements are just that, compensation, and are subject to their own inherent limitations. Balancing should be the first strategy employed during design, system integration, and correcting stabilization problems. Balancing allows the designers many other benefits. Among them; the ability to manage their mass and power budgets by using smaller torque motors, by reducing the counter torque power required to control any disturbances, thus increasing loiter time. It also enables higher slew rates without tracking degradation. And, as the result of obtaining reduced jitter image streams, balancing helps achieve more efficient video data compression.

2. MASS PROPERTIES, STATIC BALANCE

2.1 Static unbalance, acceleration, and torque

To consider Center of Gravity (CG) let's take a look at fig. 1 (below). A single degree of freedom (SDOF) gimbal is represented as viewed from the top in fig. 1a. The gimbal assembly in this case is represented by a homogeneous rectangular block with a pivot (Azimuth axis) through its geometric center. The z axis is parallel to the pivot into the paper. When an offset mass is added (fig. 1b), the center of gravity of the total assembly is moved away from the pivot and toward the added mass and the gimbal is considered unbalanced relative to the pivot. When acceleration is applied to the base plate in the direction shown in fig. 1c, the acceleration reacts through the offset CG and produces a torque about the pivot which tries to rotate the gimbal off its Line Of Sight (LOS). The amount of torque produced in this case

is equal to the product of the total weight of the moving assembly, the distance from the perpendicular line of action through the CG, and the acceleration in G as shown in fig. 1c. Relatively benign translational motion has now been transformed into more problematic torque due to the presence of this offset CG. If sufficient counter torque is not available, the gimbal responds by involuntary rotation contrary to its commanded position. The gimbal responds in the way described because it is a restrained system. If the body in question were a free body, the acceleration field would act solely through its CG and produce translation rather than rotation.

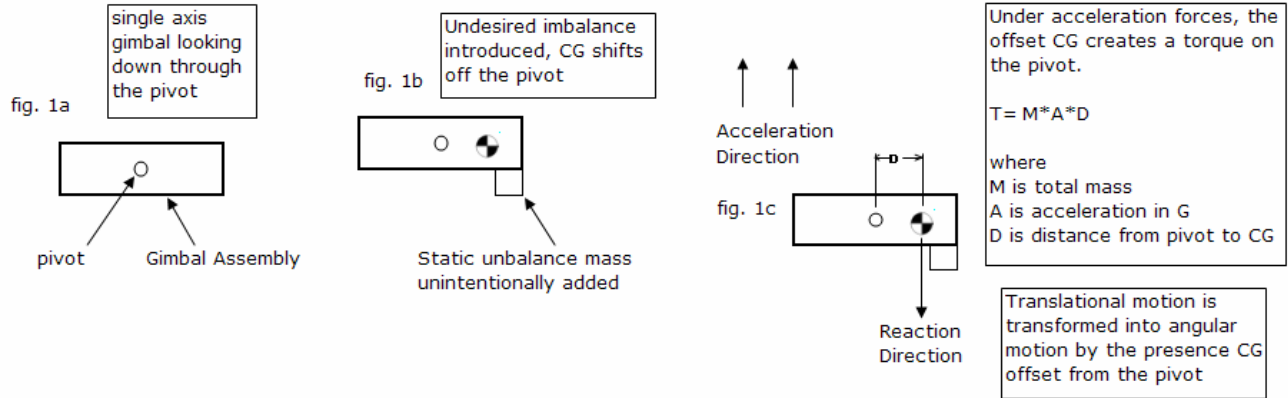


Figure 1. How torque is generated by acceleration acting on a center of gravity offset from the pivot.

2.2 Servo counter torque disturbance rejection and balance

In fig. 2 (right), a spring-damper (conceptual) is added to demonstrate the function of a servo controlled, pointing and stabilization mechanism. The drive stiffness of the servo dictates the level of counter-torque available to reject a disturbance caused by acceleration acting upon the CG offset.

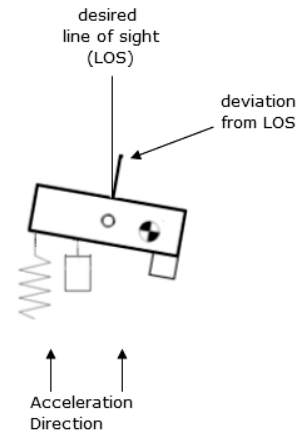


Figure 2. CG caused LOS deviation

The actual LOS deviates from the desired LOS under acceleration forces. In our simple model, if a known torque due to acceleration is counteracted by the known disturbance rejection characteristics of the servo, we can then determine how much the LOS variance will be from the commanded LOS position. An example; at a given point in time, if the instantaneous acceleration induced torque is 0.5 lb-in, and the servo has a torsional stiffness of 100 lb-in/radian, the gimbal axis will undesirably rotate through an angle of 5 mrad (assuming that response time is not a limitation).

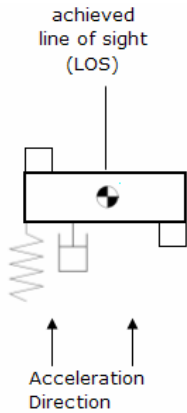


Fig. 3 Balanced

Next, a balance correction mass is added equal and opposite the initial unbalance mass (fig. 3). This pulls the CG back to the center where it is coincident with the pivot axis. With the distance-term of the torque calculation reduced to zero, and there is no remaining torque trying to deflect the gimbal from its LOS.

2.3 Degrees of freedom and off axis forces

Most vibration environments are characterized as 6 DOF; three of translational motion and three as angular motion. The frequencies and amplitudes are a mix of Gaussian random combined with non-Gaussian periodic components such as the throb of an internal combustion piston engine or the beating of a propeller. The angular degrees of freedom have little direct effect on the gimbal's reaction to a static unbalance; in this case, the mass properties driven response is mainly governed by inertia which serves to keep the gimbal pointed where it is. The modeled gimbal primarily responds to the three degrees of translational motion. In our model (fig. 4), the vector from the pivot to the CG relative to the direction of the acceleration force dictates how the unbalanced gimbal reacts. In this case shown in fig. 4a, the CG is in the acceleration "shadow" of the pivot

and imparts no torque on the pivot. So far the model has considered unidirectional motion. Poly-directional random-like vibrations have an imprecise effect on a single axis gimbal. In the 3 DOF translational diagram shown in fig. 4b, X acceleration has major torque effect mitigated somewhat by the slight off-angle gimbal axis orientation. The amount of torque reduction is related to the cosine of the angle between the acceleration direction and the axis formed by the CG and pivot. Similarly, Y acceleration has a small effect as the orientation places the CG closer to the pivot's shadow. Naturally as the acceleration direction reverses the reaction torque about the pivot will reverse. The obvious implication here is that all three axes of translational motion occur simultaneously with perhaps one of them dominant. A visualization of asymmetric 3 DOF would be to think of the three dimensional vibration magnitude envelope as represented by an oblate (flattened) spheroid. This sphere-like motion envelope acts upon a multi-axis gimbal whose CG locations are expected to change relationship to the forces as the gimbal articulates while in performance of its job. In the process the gimbal can appear steady under some positions but not others.

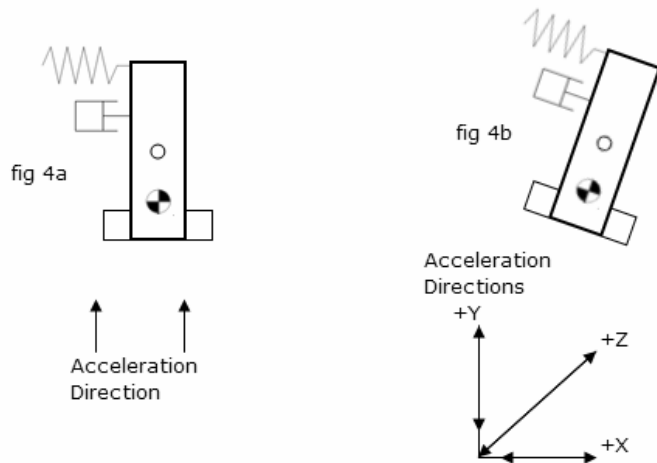


Figure 4. Acceleration vector relative to CG and pivot axis

3. JITTER

3.1 A simplified vibration profile model

Complex vibration environments are described in terms of Acceleration Spectral Density (ASD). This is analogous to a Power Spectrum. A plot of the ASD would show the power along the Y axis expressed in G^2/Hz where Hz is the bandwidth¹. The X axis would show the Frequency component of vibration in Hz. When analyzing the interplay with mass properties unbalance, it is easier to stay within the amplitude domain and think of the Y axis in G rms with G being multiples of gravity. The adaptation from G^2/Hz vs. F, to G rms vs. F, is done by selecting a meaningful bandwidth as it applies to a region of interest such as around the primary beat frequency of a helicopter's main rotor and calculating the area under the ASD curve residing between the lower frequency and the upper. The square root of this area is equal to the G rms acceleration². The value obtained is meaningful at the center of the selected frequency of interest only for the relevant bandwidth given.

3.2 Isolation, resonance, and acceleration as seen by the gimbal

Imaging gimbals are more complex than shown in fig. 2. Aside from the addition of extra rotational axes, the gimbals are frequently decoupled from the vibration environment by an isolation system. This system has its own transfer function complete with resonance. Added to the isolation resonance are the various resonances of the gimbal structure. The isolation system has another characteristic where, if the CG of the total gimbal assembly is not at the elastic center of isolation, the offset can create a modal transformation where the translational motion becomes, in part, a rocking motion³. These functions combine in an interactive way to dramatically change the amplitude and phase experienced by the craft to something very different experienced by the gimbal.

3.3 Torque on the pivot and servo dynamic stiffness

The Grms vs. frequency (bandwidth dependent) profile as seen by the gimbal can be applied to the CG moment to calculate expected disturbance torque vs. frequency. Servo disturbance rejection characteristics can be described in units of lb-in/radian of control torque (counter torque) vs. frequency. Disturbance torque (lb-in) and disturbance rejection (lb-in/rad) are used to calculate jitter motion in radians or more suitably milliradians (mrad). Using G rms indicates what performance is to be expected on average. The reality is that regular peak g forces several times the rms values are occurring. Vibration testing often sets the peak levels to that of three to five sigma peaks⁴. Depending on the application these peaks can be relevant placing a greater demand on the disturbance rejection.

It is worth mentioning that hysteresis, backlash, or similar effects create windows of opportunities for disturbance forces to transfer relatively unimpeded directly to axes, bypassing the stability loop of the gimbal. Although not modeled here, these areas of low stiffness can become the dominant jitter source in an otherwise sound system. This is an example of where balance becomes the primary tool and the only certain tool available to fight jitter.

Taken conceptually for a given excitation frequency band, the operational accelerations experienced by the aircraft are multiplied by transmissibility transfer function of the isolation system to yield an approximation of the accelerations as felt by the gimbal. The on-gimbal accelerations “amplify” any residual CG moment offset and generate a disturbance torque. This torque is divided into the disturbance rejection characterization of the control system and produces an angular jitter motion.

3.4 Jitter and MTF (image contrast)

The jitter motion will manifest itself as image blur reducing image resolution which is a function of spatial resolution and contrast. Optical system component resolutions are characterized in terms of their modular transfer function (MTF). Every part of an imaging system acts as a low pass filter reducing the higher spatial frequency components of the image and reducing the resolution. The optics, sensor, electronics, transmission, and display all have a degrading effect on the high frequencies. Other factors such as motion blurring, of which jitter blur is a component, cause even more degradation. A rule of thumb states that if jitter blur (Gaussian) is more than 10% of a pixel it has a deleterious effect on MTF⁵. The dominant effect

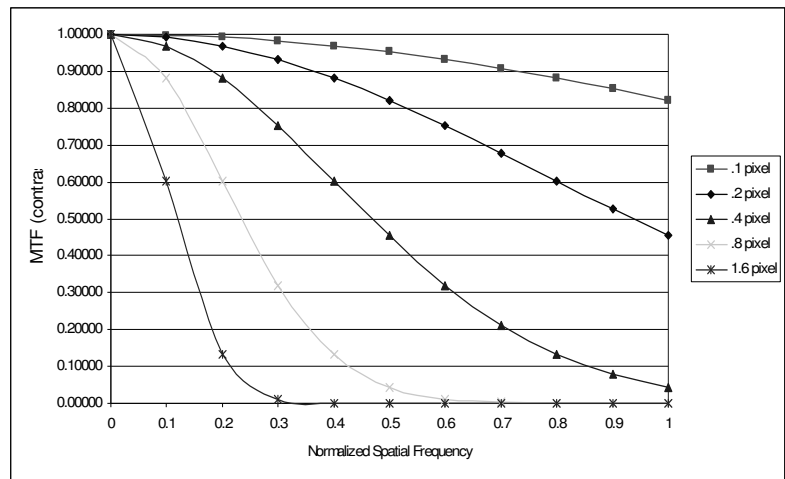


Figure 5 MTF as it relates to pixel jitter blur

depends on whether the system is considered primarily detector limited or optical limited. The assumption here is that the system is a live video feed where the observer’s perceived resolution where the eye/brain integration time is longer than the individual frame or field exposure integration time. In systems where a post capture image processing is used, or when software algorithms are used to register the frames; it is still important to limit the jitter blur within the exposure integration time.

The jitter motion relates to the MTF by comparing the field of view of a single pixel in mrad to the jitter motion in mrad. One way to express this relationship is in fractions of a pixel blur; meaning that if the motion in mrad was one-half of the FOV of the pixel, the pixel blur would be said as .5 pixels. Examining the chart in fig 5.⁶ and following the 0.4 pixel series, we see that 90 percent of the contrast is lost at 85 percent of the maximum spatial frequency. Note that the chart only shows the contribution to detector MTF degradation due to jitter motion. The jitter MTF becomes one of many transfer functions that are multiplied together to obtain the total system resolution characterization.

4. MASS PROPERTIES, DYNAMIC UNBALANCE

4.1 Product of Inertia

Dynamic unbalance is the result of a non-symmetrical mass distribution called Product of Inertia (POI). In fig 6 we see a homogeneous perfectly balanced cylinder to which two equal point masses have been attached 180 degrees apart and spaced along its length equidistant from the CG. These additional masses will not alter the CG location and the cylinder remains statically balanced.

However, the cylinder now has a POI equal to: $POI = 2 * M * R * L$

Where:

M = mass

R = radial offset distance of the mass from the cylinder centerline

L = the axial offset of the mass from the cylinder CG.

If we spin the cylinder about its vertical (Z) axis, centrifugal force acts through the two weights to produce a couple. If the cylinder is a free body spinning in space, the axis of rotation of the cylinder tilts slightly toward weights so the centrifugal forces on the weights are offset by centrifugal forces on the now unsymmetrical, tilted, cylinder. The cylinder, which, if spinning, appears to wobble, is now actually balanced statically and dynamically about its new axis of rotation. The new axis is called a principal axis. For any object there exists a principal axis coordinate system whose characteristics are;

One axis is the axis about which the Moment of Inertia (MOI) is the maximum for the object

A second axis, perpendicular to the first, is the axis about which the MOI of the object is a minimum

The third axis is perpendicular to the other two

There is no POI relative to this coordinate system

The last illustration of figure 6 treats the rotor as though it were the inner (Elevation) axis assembly of a gimbal which is rotated about the Azimuth axis. Unlike the free body example where the rotation axis tilted to relieve the centrifugal forces, the motion is now constrained by the Elevation axis torque motors trying to keep the assembly on its LOS.

The amount of centrifugal force is directly related to the rotational velocity squared. The orientation of the plane of the POI relative to the axes affects the forces similar to how a static CG unbalance relates to the pivot. Taking the worst case, where the POI plane is perpendicular to the pivot (Elevation) axis and is aligned with the rotation (Azimuth) axis, as in fig 6, the forces are calculated by the following equation⁷.

$$(lbs) F_1 = \frac{W_1 \times R_1 \times (RPM)^2}{35207}$$

Where:
 W_1 = weight of unbalance mass in lbs
 R_1 = radius of CG of unbalance in inches
 RPM = speed of rotation in RPM
 35207 = constant to transform units

To convert this centrifugal force into a torque we would multiply the force (lbs) generated by the single weight by the axial offset from CG (inches) producing a torque (lb-in). Since there are two weights making up the pure couple we double the torque.

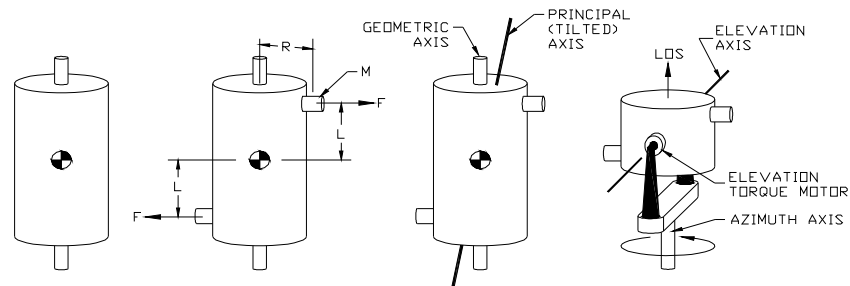


Figure 6 From balanced rotor to pure couple rotation system

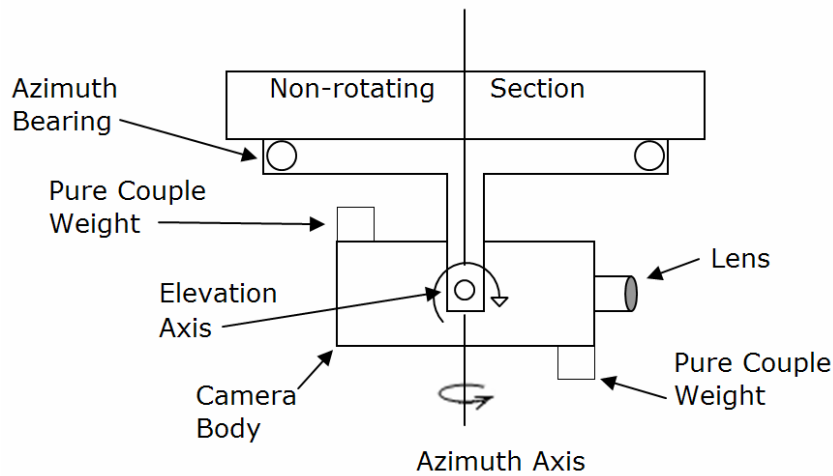


Figure 7. POI as it relates to a typical gimbal

Rarely, if at all, will a gimbal be asked to rotate continuously, at say, 30 rpm. However, it may be expected to slew 180 degrees per second, or it may experience high peak angular velocities in response to the vibration environment it is subject to. Moving from the restrained rotor example as shown in fig 6 to the gimbal example shown in fig 7, pictured is an Azimuth / Elevation gimbal that has been statically balanced but still has a dynamic unbalance. When the Azimuth axis is rapidly slewed or when it undergoes some other sort of rapid angular acceleration, the Elevation axis, in turn, attempts to rotate; just as in the restrained rotor example. The effect on

one axis by the rotation of another is what is called cross-coupling effect or cross-product effect. A reasonable strategy for dealing with this dynamic unbalance might seem to be to mount the opposite pure couple by attaching similar weights across from the offending pure couple. Although this might help, it does not eliminate POI and the cross-product effects. To understand why, we'll look at fig 8.

In the first view, the cross sectional view of the restrained rotor is shown. In the second view, correction weights have been added to cancel the original dynamic unbalance. In the third view, the rotor has been tilted. In the fourth view, the rotor was cut in half. Each half has a CG location. In the fifth view, the rotor is reassembled with the correction weights omitted. Three CG symbols represent the mass distribution of each half plus the whole. The restrained rotor is asked to spin about the axis shown. Notice how the CG pattern in the last view is similar to the first view.

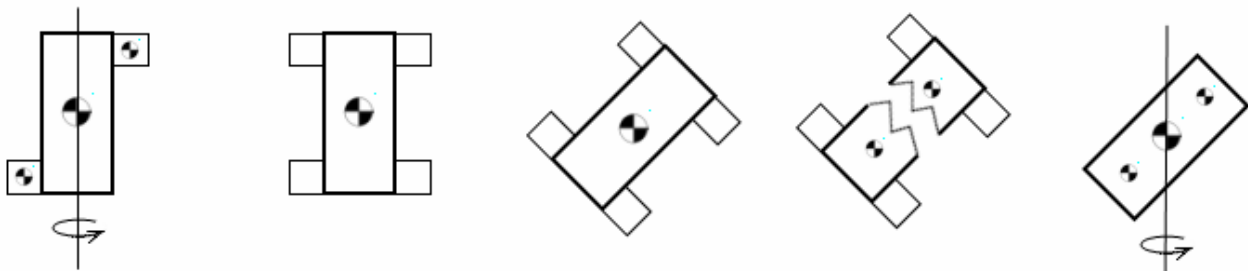


Figure 8. Why dynamic balance is not balanced in all orientations

This is because the camera body coordinate system has tilted relative to the Azimuth axis. If we consider a new camera body coordinate system where one axis is parallel to the Azimuth axis, we find that POI does exist, purely due to the tilt. This is always true unless the camera has the mass properties of a sphere, cube, or a round or square cylinder with the Elevation axis being the axis of symmetry.

4.2 Spheres, Cubes, and Squares

The only way to resolve the fig 8 dilemma is to make the moment of inertias about all axes through the CG, that are perpendicular to the Elevation axis, equal to each other. Consider a homogeneous sphere. It has no static or dynamic unbalance. It has no specific principal axis. Any and all axes are principal axes. No matter what acceleration or motion is imparted to it, it does not show any cross-product reaction. Similarly a homogenous cube has the same characteristics; the MOIs about any axis through the CG (which is at the gimbal axes intersection) are equal no matter which way you

twist it. In our restrained axis gimbal systems, it is valid to simplify these principals further and imagine final relevant MOI matching to take the mass properties form of a square or round cylinder with the Elevation axis being the axis of symmetry. As discussed later the degree of MOI matching required is highly dependent on the performance criteria of the gimbal. MOI matching is best accomplished in the early design phase of the gimbal when components can be moved relatively easy to minimize ballast requirements during final balance.

4.3 Elevation's effect on Azimuth

The examples demonstrated thus far are where the Elevation axis is excited by the rotation of Azimuth. However, if a POI resides on the Elevation and the Elevation axis slews quickly or vibrates, it could have a cross-product effect on Azimuth. The Azimuth axis static balance is critical for all the reasons mentioned for Elevation. However when considering cross product effects, the Azimuth can tolerate a dynamic unbalance. A POI on Azimuth cannot cross-couple to Elevation in the same way as described earlier. It can however, work against the axial stiffness of its own bearings causing unanticipated force which attempt to violate the restraint and may cause premature bearing wear.

5. STRATEGIES AND METHODS

5.1 Strategies

Ideally we would like to create a method which involves making a measurement, calculating a correction, and achieving the improvement expected. To accomplish these goals we have to consider several factors.

- The configuration of the gimbal
- The initial unbalances
- The tare mass and moment distribution of holding fixtures
- The level of disassembly allowed
- The repeatability of the reassembly process
- The sensitivity of, and type of equipment available

A complicating factor is the actual ability to physically and accurately place correction weights where they are needed to be most effective and to hold the overall balance solution to minimum added mass. At the highest level the strategy is to static balance first, dynamic balance second, inertia match third, then to verify the static balance as the last step. This process recognizes the physical limitations of even the world's most sensitive direct-measuring machines and methods.

5.2 Methods

Ideally, to statically balance a gimbal would be to quickly and accurately measure the unbalance quantitatively, determine the amount and location of ballast weights required, mount the ballast, then re-measure to confirm that balance has been achieved. The method which comes closest to achieving this goal is to use a dedicated two axis force rebalance gimbal balance instrument.

On a dedicated two axis force rebalance gimbal balance instrument, the fully assembled gimbal is mounted on a dedicated fixture which orients the 2 gimbal axes in a vertical plane, each at 45° to the horizontal⁸. This allows making four unbalance measurements in one setup from which the unbalance about both axes can be determined. The gimbal drive/read control system is often utilized to fully automate the process. Measurement time is typically under 2 minutes. With the high sensitivity and accuracy, unbalance reduction ratios on the order of 95% are typically achieved. If ballast can be accurately mounted on the gimbal, balance within tolerance can often be achieved in one pass. Ideally, the gimbal is left on the instrument during ballasting so balance can be quickly confirmed or a second iteration performed if necessary. With a good weight correction configuration, a good selection program, and a skilled operator, a gimbal can be balanced within ½ hour.

With sensitivity approaching 0.1 gm-cm they are most suitable for gimbals with very tight balance requirements and small allowable rotation angles. All other methods, while usually less expensive, are less accurate and more time consuming.

All methods can benefit from a well defined weight correction plan. A well thought out plan can decrease the calculation process necessary to determine the proper weight placement and mass amounts to correct the measured static unbalance. Hand calculation of these correction weights can be complex and often results in correcting one axis for ballast previously mounted to correct the unbalance about another axis. A properly configured correction weight analysis program can simultaneously track all the axes unbalances and select the best configuration of weights based on the measured unbalances and the correction weight effects. The program should be capable of minimizing added ballast and tracking/managing POI during the solution build-up.

As with static unbalance several methods can be used to measure and correct the dynamic unbalance of a gimbal including a half-dozen variants of measuring either MOI directly or POI directly. The achievable results of each these techniques can vary greatly depending on the gimbals' compatibility with the process. One technique may require the gimbal to be disassembled while others require the gimbal to have the ability to rotate a full 360 about its own bearing assembly. Gimbals can be balanced using a single technique or a mix of these techniques.

Dynamic POI measurements have the advantage of amplifying the affects of the dynamic unbalances by increasing the spin rate of the dynamic balance machine. Also, since the POI unbalances throughout the process can be iteratively corrected, and since the uncertainties are a function of the total unbalance, the accuracy can be maximized. With the MOI approach, every gimbal will have parasitic MOI that exists due to fixtures and other gimbal structures. This parasitic MOI increases the overall MOI being measured. Since the accuracy of MOI measurement is a function of total MOI under test, the uncertainty of measurement escalates with increasing MOI, further decreasing the capability to measure and correct balance.

The first and most accurate method of dynamic unbalance measurement is only applicable for a specific gimbal type. This measurement technique uses the gimbal's own bearings and motor control assembly to spin the gimbal for dynamic measurement of the unbalance. To be compatible with this method, gimbals must be able to rotate a full 360 degrees about their rotational axes for an unlimited number of rotations. A vertical 2 plane non-rotating dynamic balancer is used to measure the dynamic forces generated by the unbalances while the gimbal is under rotation. The gimbal will be configured in several orientations for these measurements and the resulting measured unbalances are corrected.

Another method that works similar to the first is to use a vertical 2 plane rotating dynamic balancer and hold the gimbal at various angles during the series of tests. This system gets the performance benefits of the spin method with gimbals that do not meet the full 360 degrees rotation requirement. The effectiveness of this method decreases with gimbals that have small travel angles (below ± 15 degrees). The outer assembly of the gimbal is under rotation along with the inner assemblies. In order to optimize the measurement performance, these parasitic assemblies must be statically and dynamically balanced in order to not mask the delta unbalances of the unknown inner axis. New methods for measuring and correction using a two-plane balancer are described later in this paper.

The next method is the best for design engineering evaluation and not very practical for production testing. During manufacturing, the gimbal inner axis assembly is placed on a spin balance machine and the POI is measured. The gimbal is mounted in several orientations to measure and correct the dynamic unbalance. Since this method measures the gimbal assembly alone with no other interacting masses it is the most accurate if the axis assembly under test could be used alone. However since the gimbal is disassembled, this technique does not take into account any assembly components that connect between the inner and outer assemblies (cables, coolant lines, etc). Since these components often cannot be held to mass and position tolerances so that their mass properties are known and repeatable, they will add to the overall uncertainty.

Another method of measuring the dynamic unbalance uses Mohr's circle to utilize a series of MOI measurements to determine the dynamic unbalance of the assembly and correct this unbalance⁹. To collect all the necessary MOI

measurements to perform the calculations, 6 to 9 MOI measurements per axis must be made. These measurements must be performed with the MOI measurement machine's oscillation axis coincident with the intersection of the rotational axes of the gimbal, and the measurement machine's oscillation axis in the plane of POI unbalance. Since the process can be done with a fully assembled gimbal, it is not subject to the uncertainty due to missing assembly masses as in previous methods. However, this advantage creates an error source of its own. Since the outer assembly and frame assembly all are mounted on the measurement system, the overall inertia being measured is high relative to the delta MOI being measured. This creates a large percentage uncertainty which may dramatically reduce the accuracy of this method. The process is performed on a fully assembled gimbal so it is compatible with both engineering and production environments, however the high number of MOI measurements required makes it slow and less attractive for production use.

5.3 MOI Matching

As noted earlier, compensating for POI in a given orientation does not necessarily eliminate the dynamic unbalance problem. If the assembly being balanced does not have the mass properties of a square or round cylinder, tilting it will generate a new POI. The next step in the balancing process would be to add ballast to increase the MOI about the axis of minimum MOI to match the MOI of the axis of maximum MOI. This would reduce the POI due to tilt to zero. Unless the original design of the gimbal had this feature as a design goal, the required ballast mass and resulting MOI might very well degrade the gimbal performance.

5.4 New process for dynamic balancing

New methods for dynamically balancing gimbal assemblies are under development. Previous methods using spin balance machines did not balance all POI planes and usually found balance solutions valid for gimbals pointed straight ahead (boresight). In the newly developing methods, through the use of multiple position fixturing, all POI planes are exposed for measurement and correction. The following describes the highlights of one of the processes as it was tested at Space Electronics.

At the time of this process development, the ideal machine, a POI-50, was not available. A POI-50 is a two-plane dynamic spin balance machine with a 50 lb payload capacity. The only two-plane balancer readily available was a POI-2200 (2200 lb payload capacity) with a 50 rpm sensitivity rating of 0.5 lb-in² as opposed to the POI-50 with sensitivity of 0.07 lb-in². If we replaced our standard test gimbal with a scaled up version with appropriately scaled up unbalances, we could verify balancing process and math involved. To that end, we adapted a POI testing jig to function as a 2 axis gimbal. A 50 rpm spin speed was chosen in order to obtain forces high enough to measure while staying well below speeds which might cause damage to a typical gimbal. Knowing the limitations of the equipment involved we feel confident that the principles, as shown, are certain to scale downward when applied to operational gimbals.

The new "gimbal" Azimuth axis assembly weighed about 5 lbs and its Elevation axis assembly about 30 lbs. We intentionally added a 48 lb-in static CG offset and a dynamic unbalance. By using such exaggerated unbalances we were able to rise above the sensitivity noise floor of the POI2200. The static unbalance was created by adding three masses to the gimbal in such a way that each created an independent CG offset along the X, Y, or Z axis of the Elevation assembly.

The Large Test Gimbal (LTG) unbalance was first statically measured using a GM904 gimbal balance machine. The balance tolerance for this initial test was kept loose, slightly less than 0.9 lb-in and well above the machine's 0.0006 lb-in sensitivity capability, in recognition of the scaled-up assembly. The intent of static balancing is to leave only a residual POI unbalance which can be modeled as a pure couple. After easily obtaining the static tolerance using well established methods, the LTG was brought to the POI machine¹⁰.

The first mounting orientation (fig. 9) was designed to expose the POI P_{ZX} and P_{ZY} planes of the Elevation axis for measurement. The LTG was oriented with the Elevation axis vertical and the Azimuth axis horizontal by using an L-fixture. The Azimuth axis was locked down after ensuring the Elevation axis was indeed vertical. The Elevation was positioned at one travel extreme and also locked. The next step was to correct for the large fixturing unbalances by incrementally measuring and correcting at increasing speeds until 50 rpm at a high gain setting was reached. First, by the addition of several lbs of CG correction and later by the addition of POI weights, the entire machine spindle and

fixture was balanced. A POI Tare measurement was made at this stage. Next, the Elevation axis was rotated 180 degrees (work reversal) to its other travel extreme and locked.

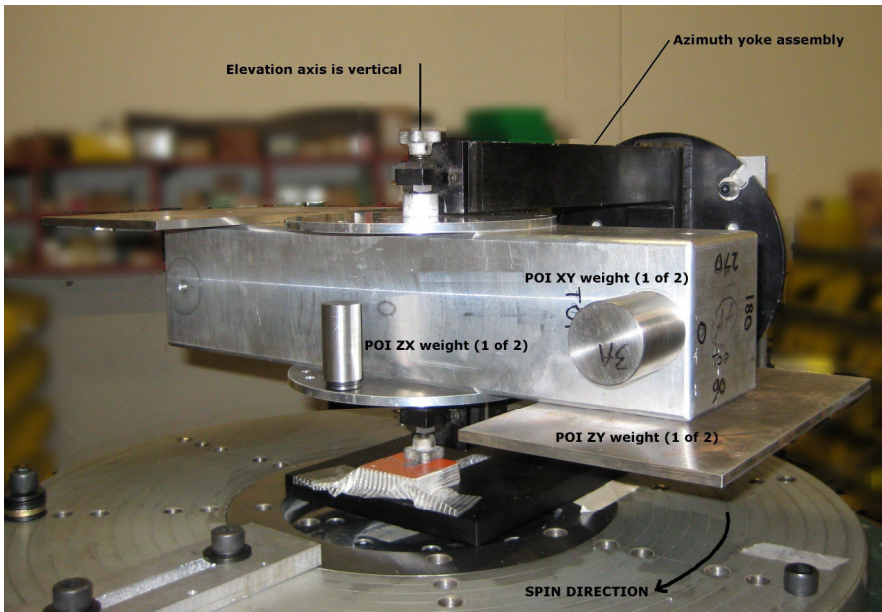


Figure 9. POI measurement of elevation assembly – P_{ZX} and P_{ZY}

A POI Part measurement was obtained in this position (fig. 9). The P_{ZY} value of 290.06 lb-in², and a P_{ZX} value of 8.14 lb-in² was calculated by the POI2200 controlling computer. The measured P_{ZY} value was within 0.1% of the predicted value. Both the measured value and the predicted value are a factor of two greater than the actual POI because we used the 180° degree work-reversal method for the measurement. Given that P_{ZY} represented the lion's share of the unbalance, and the measurement method yielded twice the real unbalance, we corrected P_{ZY} by making half the indicated correction to the Elevation assembly.

The LTG Elevation axis was swung and locked back to the original travel extreme for its Tare, then brought back to the other extreme for the Part measurement. A POI calculation indicated that P_{ZY} measured -0.33 lb-in² and was deemed successfully reduced, but P_{ZX} was now dominant at 4.8 lb-in², noting that the P_{ZX} value matched the predicted value to within 2.5 %. Again, the work-reversal method yields a POI twice its real value so half the indicated correction was made to the P_{ZX} plane. The same work reversal measurement was implemented a third time yielding a residual P_{ZY} of 0.28 lb-in² and a P_{ZX} of -0.12 lb-in²; both were well within the 50 rpm sensitivity of 0.5 lb-in², this balance level indicated it was time to stop.

The LTG and L-fixture were removed along with the temporary spindle balance weights to return the machine to its bare table condition. The LTG was remounted to the POI2200 so that the Elevation axis was horizontal and the Azimuth axis was vertical (fig.10). This mounting orientation would expose the remaining previously hidden P_{XY} of the Elevation assembly, as well as the P_{ZY} and P_{ZX} of the Azimuth assembly. In this fixturing orientation, the goal was to measure POI in each of three Elevation positions and to calculate the angle and maximum POI magnitude for Elevation's P_{XY} plane. The Azimuth axis was locked so that the Elevation axis was parallel to the machine Y-axis. The Elevation axis was locked with the LTG looking vertical. As before, incrementally increasing speed measurements, calculations, and corrections were made to prebalance the machine's spindle and fixture to increase the signal to noise ratio. A POI Tare measurement was now run.

With the Elevation axis LOS still vertical (we'll call it 0-deg) a POI Part measurement was run and calculated against the recently run Tare. Since the Elevation assembly's P_{ZY} plane is parallel to the machine's P_{ZX} plane, we record the machine P_{ZX} measured value of 64.80 lb-in². Next, we rotated the Elevation assembly to 30-deg off vertical, lock, remeasure, and calculate. The measured P_{ZX} value of -339.57 lb-in² was recorded. Finally, the Elevation axis was rotated to 90-deg off vertical, locked, and remeasured, with a resulting of P_{ZX} of -65.12 lb-in².

The three P_{ZX} measurements are entered into a matrix calculator that takes the three POI points and fits them to a sine curve which yields a calculated Elevation-assembly peak P_{XY} magnitude of 433.1 lb-in² at 139-deg relative to the LOS vertical position. With the maximum POI identified, we use the strategy of reducing that maximum POI to zero and thus by default obtain matching MOIs and zeroing POI for all Elevation orientations.

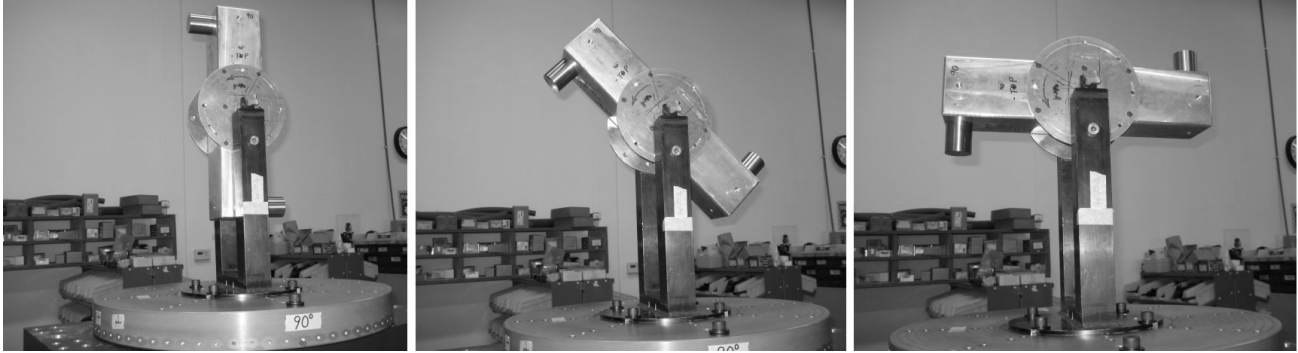


Figure 10. POI measurement of elevation assembly P_{XY} in three positions 0, 30, and 90 degrees

Theory

Mohr's circle shows that the diameter of the circle is equal to;

$$I_d = I_{mx} - I_{mn}$$

the difference between the maximum MOI and minimum MOI. The axes about which MOI is maximum and minimum are Principal axes and the POI is zero.

The maximum POI (P_m) occurs relative to an axis at 45° between the principal axes. The magnitude of the POI is the radius of the circle.

$$P_m = I_d/2$$

If the difference between the maximum and minimum MOI is driven to zero, the circle diameter becomes zero and there can be no POI relative to any axis.

Method

1. Find the maximum POI magnitude (P_m) and its angular orientation of its axis relative to the gimbal coordinate system. At $\pm 45^\circ$ to this axis will be principal axes about which MOI is Maximum (I_{mx}) and Minimum (I_{mn}).

2. Add ballast to make the Min MOI and Max MOI equal or $I_d = 0$.

$$I_d = 0 = 2P_m \text{ therefore } P_m = 0$$

Select a suitable radius (R) within the gimbal envelope. Two masses (M) are required for MOI matching. $M = P_m/R^2$.

process during the production phase. Simple modeling cannot come close to describing the breadth of what is necessary to properly consider the POI problem. The many variables suggest that a reasonable course of action is to measure and correct POI; then to quantitatively analyze the MTF results by operating the gimbal assembly in a meaningful vibration environment.

Reducing the effects of dynamic unbalance is a far more costly and time consuming to be practical as a production line process, and is likely to be secondary to static in all but the most advanced gimbals. Incorporating MOI matching and minimum POI in the initial design then verifying the design by measuring the first few units is likely to be far more cost effective than trying to reduce POI and alter MOI on the completed production gimbal. A place exists for post-design dynamic balancing when evaluating legacy gimbals and when repairing or upgrading gimbals during life extension programs. To accommodate any scenario's requirement to dynamic balance, new methods are available that address all the concerns regarding the limitations of formerly used processes.

7. ACKNOWLEDGEMENTS

We would like to thank Robert Bell, Paul Kennedy, and Camille Marquis of Space Electronics for their valuable input.

REFERENCES

- [1] Irvine, T., "Power Spectral Density Units - Rev B", *Vibrationdata*, pp. 1 (March 2007).
- [2] Irvine, T., "Power Spectral Density Units - Rev B", *Vibrationdata*, pp. 6-7 (March 2007).
- [3] Andrews, F. J., "A Primer for Vibration Isolation", *Fabreeka International.*, (February 2008), http://www.fabreeka.com/tech/Primer_Vibr_Isol.pdf
- [4] Van Baren, J., "How to get peaks back into 120G random profile", *Test Engineering and Measurement*, Oakland, CA., August/September 2007.
- [5] Holst, G. C., *CCD Arrays Cameras and Displays*, JCD Publishing / SPIE Press, Bellingham, WA., pp. 252 (1996)
- [6] Holst, G. C., *CCD Arrays Cameras and Displays*, JCD Publishing / SPIE Press, Bellingham, WA., pp. 252-253 (1996) – used formulas and graph concept.
- [7] Boynton, R. and Wiener, K., "Mass Properties Handbook", *Society of Allied Weight Engineers*, La Mesa, CA., No. 2444, pp. 53, (May 1998)
- [8] Boynton, R., Wiener, K., Kennedy, P., and Rathbun, B., "Static Balancing a Device with Two or More Degrees of Freedom", *Society of Allied Weight Engineers*, La Mesa, CA., No. 3320, pp. 12-14, (May 2003)
- [9] Wiener, K. and Boynton, R., "Using the Moment of Inertia Method to Determine Product of Inertia", *Society of Allied Weight Engineers*, La Mesa, CA., No. 2093, (May 2003)
- [10] Boynton, R., Wiener, K., Kennedy, P., and Rathbun, B., "Static Balancing a Device with Two or More Degrees of Freedom", *Society of Allied Weight Engineers*, La Mesa, CA., No. 3320, pp. 12-14, (May 2003)